ACS APPLIED POLYMER MATERIALS

pubs.acs.org/acsapm Article

Continuous Processing of Cellulose Nanofibril Sheets Through Conventional Single-Screw Extrusion

Sami M. El Awad Azrak, William J. Costakis, Robert J. Moon, Gregory T. Schueneman, and Jeffrey P. Youngblood*

Cite This: *ACS Appl. Polym. Mater.* 2020, 2, 3365−3377 Read Online

ACCESS | Metrics & More | Article Recommendations | Supporting Information

ABSTRACT: Extrusion-based processes are one of the most widely used continuous polymer processing techniques because of their commercial availability, versatility, and cost-effective scalability. For these reasons, conventional single-screw extrusion was investigated and used for continuously processing mechanically fibrillated cellulose nanofibrils (CNFs) into wet sheets. A high shear mixing procedure was used to process highly loaded CNF pastes with up to ∼25 wt % solids, composed of ∼91 wt % CNF and ≤ ∼9 wt % of a processing aid like carboxymethyl cellulose (CMC), xanthan gum (XG), or anionic polyacrylamide (aPAM). Validation of the mixing procedure proved that highly loaded CNF/processing aid pastes can be processed in under 40 min. The higher solid loadings significantly reduced the preparation and drying time. The water-retention ability and stability of CNF suspensions containing different processing aids were assessed through centrifugation and zeta potential analysis. Extrusion of the prepared pastes showed that cohesive sheets could be produced continuously at output rates of 7.45 ± 0.47 kg/h (or 1.14 ± 0.072 dry) without the introduction of surface defects. Wet extrudates with an average width of ∼5 cm and thickness of 1.46 ± 0.05 mm were continuously processed, with the length limited only by the lack of collection rolls. A viscosity−shear rate dependence analysis linked extrudate homogeneity and reduced defects to a stronger Newtonian response for CNF/CMC pastes when compared to pure CNFs. On the other hand, CNF/XG and CNF/aPAM pastes experienced a much stronger shear thinning response, which correlated with a stronger appearance of observable aggregates and pinhole defects in the extrudates. Tensile testing of the pressed and heated CNF/CMC extrudates revealed equivalent mechanical properties to cast CNF films prepared through conventional solution casting. Lastly, preliminary calendering results for CNF/CMC extrudates showed that full consolidation can be achieved, thus providing a way to continuously dry and press the wet extrudates.

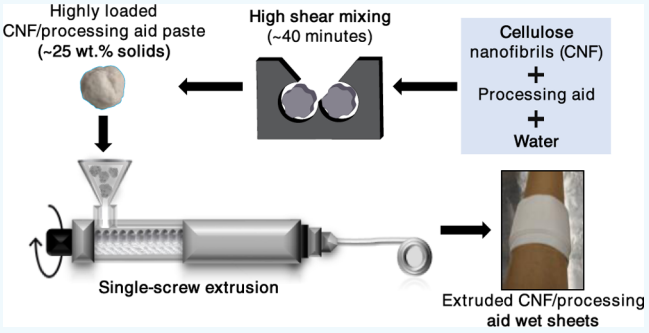

KEYWORDS: *nanocellulose, extrusion, carboxymethyl-cellulose, CNF, torque rheometer*

INTRODUCTION

The concept of a circular economy has been used across various industries to conceptualize the balance between economic benefits with resource scarcity and environmental impact.[1−3] Cellulose-based materials are a natural fit to this approach as they are inexpensive, plentiful, and can have minimal environmental impact (e.g., nontoxic, biodegradable, facilitating the sequestration of CO_2) and as a consequence are prolific within our society, as demonstrated by the enormity of the worldwide industries in cellulose derivatives, paper/packaging, textiles, and forest products. Cellulose is a highly functionalizable polymer; when these chains are bundled together forming highly ordered domains that can be subsequently extracted as nanoparticles, they exhibit unique characteristics because of their nanoscale size, fibril morphology, and large surface area.[4−6] These cellulose-based nanoparticles, generically called cellulose nanomaterials (CNMs), have properties and functionalities distinct from molecular cellulose and wood pulp, and thus give new cellulose material utilization opportunities,[7] such as nanocomposite materials.[8] There are many types of CNMs depending on the cellulose source material, nanoparticle production process, and resulting surface chemistry.[4,7,9] The current study focuses on cellulose nanofibrils (CNFs), which are produced by mechanically fibrillating wood pulp, where the resulting particles are flexible, with a high aspect ratio, fibril morphology, a degree of branching (e.g., a thicker central fibril with thinner fibrils extending off), and a strong tendency of forming open network/aggregated structures.

Received: May 4, 2020
Accepted: June 25, 2020
Published: June 25, 2020

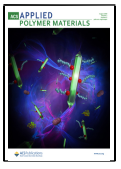

https://dx.doi.org/10.1021/acsapm.0c00477
ACS Appl. Polym. Mater. 2020, 2, 3365−3377

CNM properties are not necessarily unique when compared to inorganic nanoparticles; however, unlike other nanoparticle materials, CNMs are renewable, sustainable, biodegradable, and have low/minimal environment, health, and safety risks (based on preliminary testing[10,11]), can be produced at industrial scale with relatively low costs,[12−14] and are globally sourced. Because of these facts, CNMs have become an attractive material to reduce the dependence on oil-derived synthetic polymers and has accelerated efforts to process them into useable forms like films, fibers, and coatings.[15−19] For example, multilayer CNF structures or laminates with a thickness of up to 1.65 mm have been reported, which could serve in high-strength and lightweight structural and packaging applications.[20] Even though the reported advances in CNM processing and forming are very promising, to make greater inroads for CNM utilization, further advances are needed in the development of bulk composite processing approaches for CNMs. These methods must be fast, cost-effective, and satisfy the functionality needed by the industry (e.g., mechanical, thermal, optical, etc.).

Current bulk processing of CNMs have mainly focused on the formation of cellulose nanocomposite films or sheets by compounding CNMs and a matrix polymer.[21] These methods have been successful at incorporating CNF, using a twin-screw extruder, into different polymeric matrices like thermoplastic starch, polyvinyl acetate, polylactic acid, and others.[22−25] Though successful at continuous processing, extrusion of cellulose nanocomposites is largely limited by the incompatibility between the hydrophilic reinforcing phase (e.g., CNMs) and the hydrophobic matrix (e.g., synthetic polymer). Hence, the addition of higher contents (>20 wt %) of CNMs eventually leads to aggregation, and the low contents of CNM needed for processing lower the mechanical properties of the nanocomposites.[25] Furthermore, extrusion processes typically require a meltable phase, whereas most CNMs and cellulose derivatives reach their degradation temperature (T_d) before reaching their melting temperature (T_m), which limits both the processing temperature window and the possible synthetic matrices ($T_{m,polymer\ matrix}$ < 200 °C).[26,27]

One solution to this complex processing problem is to bulk process CNMs without the use of any synthetic polymer matrix (i.e., ∼100% pure CNM structures). This eliminates incompatibility issues with hydrophobic polymer matrices and gives the ability to take full advantage of the impressive CNM properties. It also allows processing of CNM at lower temperatures. However, processing ∼100% pure CNM structures introduces new challenges, the first being the inability of pure CNMs to melt and form entangled polymer networks; hence, similar viscoelastic properties to polymer melts are hard to achieve and have not been reported. Second, because of the isolation processes used to extract CNMs, a significant amount of water is retained by CNMs (>80 wt % water) and must be removed; hence, a high hydraulic capacity is needed during processing and forming.[4] Lastly, CNM slurries are two-component materials composed of cellulose nanoparticles and water, which make the rheological control more complex during processing.[28] Although challenging, the extrusion of mostly pure CNMs will open up new ways toward bulk continuous processing that are otherwise not possible with batch-based or semiautomatic techniques currently used.

In this paper, we report both the first continuously processed wet CNF sheet using conventional single-screw extrusion and the first preparation of CNF pastes with up to ∼25 wt % solids using a shear mixer. The results showed that highly loaded CNF pastes with up to ∼25 wt % solids, composed of ∼91 wt % CNF and ≤∼9 wt % of a processing aid like carboxymethyl cellulose (CMC), xanthan gum (XG), or anionic polyacrylamide (aPAM), can be produced in under 40 min using a standard shear mixer. The higher solid loadings significantly reduced the preparation and drying time. The mixing procedure was validated against typical air drying to achieve higher solid loadings in CNF/aid pastes. The extrusion of the prepared pastes showed that cohesive sheets could be produced continuously at output rates of 7.45 ± 0.47 kg/h (or 1.14 ± 0.072 dry) without any significant introduction of surface defects. Wet extrudates with an average width of ∼5 cm and thickness of 1.46 ± 0.05 mm were continuously processed, with the length limited only by the lack of collection rolls. Tensile testing of the pressed and heated extrudates revealed equivalent mechanical properties to cast CNF films prepared through conventional solution casting. More broadly, the results presented show that it is possible to utilize common polymer processing methods for CNF from the beginning to the end of the processing chain, allowing the potential to significantly increase the processing rate and lower the cost associated with typical CNF processing.

EXPERIMENTAL SECTION

Materials. Carboxylated methyl cellulose sodium salt powder (e.g., CMC) was purchased from Alfa Aesar (Lot #R07E012, D.S 0.69, η = 660 mPa·s at 1% v/v at 25 °C, M_w ∼ 150,000 to 180,000). A copolymer of acrylamide and acrylic acid, typically referred to as aPAM, a water-in-oil type emulsion (Nalclear 7768), was kindly supplied by Nalco Water (EcoLab). The solid content of the aPAM emulsion was found to be ∼32 wt %. The average molecular weight of aPAM was not measured, but it is generally expected to be at least in the million range and has a linear molecular structure.[29] XG from *Xanthomonas campestris* was purchased from Sigma-Aldrich (Lot #SLBZ5317, η = 800 to 1200 mPa·s at 1% v/v at 25 °C, M_w was not supplied but has been reported to vary between 300,000 and 7.5 × 10^6).[30] Hydroxyethyl methyl cellulose powder (product no. 435015), hydroxyethyl cellulose powder (product no. 09368), poly(ethyleneimine) solution (50% H_2O, M_w = 750,000), and polyacrylic acid sodium salt solution (45% H_2O, M_w = 8000) were purchased from Sigma-Aldrich. Tragacanth gum powder (product no. A18502-22) and methyl cellulose powder (product no. 43483) were purchased from Alfa Aesar. Amphoteric starch powder (Chargemaster R25F, D.S. 0.027) and cationic starch powder (Chargemaster R33F, D.S 0.032) were kindly supplied by Grain Processing Corporation. Carbopol 940 was kindly supplied by Lubrizol. Carrageenan-lambda (Viscarin GP 5015) was kindly supplied by DuPont. Food-grade konjac glucomannan powder and guar gum powder were both purchased from regional stores. Mechanically fibrillated CNFs produced at the Process Development Center (PDC) were bought from University of Maine, Orono, ME, USA at two different solid concentrations, 3.1 wt % (Batch #110, 90% retained fines) and ∼23.5 wt % (Batch #122), both in water.[31] This variety of CNF is more coarse (e.g., diameter ∼ 20 to 100 nm) and branched (e.g., a thicker central fibril with thinner fibrils extending off) and often has been referenced in the literature as cellulose microfibrils (CMFs).[7] A transmission electron microscopy image of the CNF used is shown in Figure S1. The process of isolating/making the CNF slurry is explained in detail by de Assis et al.[13] This type of CNF is isolated without the use of enzymes and has been compared to other CNF materials (see ref 32 for CNF-1). The CNF was used as delivered without any surface or solvent modification/exchange and mixed with the respective processing aids at different ratios by dry weight.

Two stainless steel meshes ("Dutch Weave", 316SS) with a mesh size of 165 × 800 and two temperature-resistant silicone rubber sheets with a hardness of 60A were purchased from McMaster Carr Supply

https://dx.doi.org/10.1021/acsapm.0c00477
ACS Appl. Polym. Mater. 2020, 2, 3365−3377

Company, Elmhurst, IL, USA. Both materials were cut down to a square size of 115 × 115 mm ($L \times W$) and used for pressing the extrudates.

Preparation of CNF/Processing Aid Suspensions for Centrifugation. CNF and processing aid suspensions for centrifugation/separation column test were prepared by first fully dissolving the processing aid in water and then mixing it with a CNF slurry at 3.1 wt %. Two different dry weight ratios of the processing aid to CNF of 0.1:1 and 0.05:1 were prepared. The suspensions were shear-mixed using a SpeedMixer (Flacktek Inc.) system at 2500 rpm for 15 min. Subsequently, 35 mL of the suspensions were loaded into 50 mL centrifugation tubes (Falcon) and centrifuged (HERMLE Z300, Hermie Labortechnik GmbH, Germany) at 4500 rpm for 30 min (RCF ~ 3500). The separated water or supernatant was weighed on an analytical balance and recorded.

Preparation of Extrusion Pastes. Pure CNFs with the solid concentration of 10, 17, 20, 24, and 30 wt % were prepared by air drying an initial 3.1 wt % CNF slurry at room temperature. Following drying, the pastes were blended using a common household blender until being fully homogeneous. The pastes were then extruded.

CNF/processing aid pastes (CNF/CMC, CMC/XG, and CNF/aPAM) with a solid concentration of 15.32 wt % or greater were prepared using a high shear torque mixer (Plasti-Corder PL 2100 Electronic Torque Rheometer, C. W. Brabender, South Hackensack, NJ) equipped with Banbury-type mixing blades. Geometrical data as well as a detailed schematic of the setup are presented in other literature.[33] All the CNF/processing aid pastes were prepared by first adding 52 g of CNF with a solid concentration of ~23.5 wt % into the mixer. The added CNF was mixed at 120 rpm and a temperature of 60 °C until the output torque curve reached a plateau, which on average took ~5 to 8 min (Figure S2). After reaching the torque plateau, the required amount of processing aid was gradually added in smaller discrete steps to the paste until a ratio of 0.05:1 or 0.1:1 was reached (aid/CNF, both dry weight). It is important to note that the addition of the processing aid caused a significant drop in torque. Water was added as needed into the paste to control the final solid concentration and replace water lost during mixing (~1 wt % solid increase for a mixing time of 40 min). During mixing, the rotor speed was held at 120 rpm for CNF/CMC pastes and was lowered to 20 rpm for CNF/XG and CNF/aPAM pastes to avoid improper mixing because of the material sticking or slipping at the mixing blades. The pastes were mixed until the processing aid was fully incorporated into the paste. For all processing aids, full incorporation was signaled by a steady rise in torque and a secondary plateau (Figure S2). It is important to point out that if the torque plateaus are not reached, then the processing aid will not be fully incorporated into the CNF and the resulting pastes will have a grainy consistency (Figure S3). Samaniuk et al. investigated in more detail the relationships among torque drop, drop time, and processing aid concentration for corn stover pastes in a similar torque rheometer.[34] The total paste preparation time for a single batch (~66 g at ~15 wt %) was roughly between ~30 and 40 min, depending on how quickly the plateaus were reached (Figure S2). Unlike CMC and XG, lower concentrations for aPAM were used (0.026:1 and 0.013:1), as aPAM could not be incorporated completely at a ratio of 0.1:1 or 0.05:1 (i.e., the torque plateau will not be reached, resulting in a grainy and inhomogeneous paste, Figure S3). Video S1 shows the CNF paste behavior before and after CMC addition. A similar behavior was observed for XG and aPAM. Figure S4 shows a highly loaded paste of CNF/CMC after removal from the mixing cavity. For all concentrations, the mixing procedure was repeated three times to yield enough material to perform both extrusion and rheological analysis. Table S1 shows the different pastes prepared for extrusion.

It is important to point out that throughout this report the word "paste" will refer to CNF/processing aid mixtures, which have a high total solid content and are intended to be extruded. On the other hand, the word "suspension" will be used for aqueous-based mixtures with low total solid (≤~3 wt %) content like those used for zeta potential or gels used for centrifugation.

Solid Content Calculation. For all the suspensions and pastes processed, the total solid concentration or solid loading (wt %) was calculated by weighing roughly 1 g of the suspension, paste, or extrudate and then drying in an oven overnight (>12 h) at 110 °C with subsequent reweighing.

Preparation of Cast CNF Films. Cast CNF films were prepared by casting 40 g of a CNF/water suspension with a total solid concentration of 1 wt % into a 90 mm diameter polypropylene Petri dish. The Petri dishes were left to dry in a humidity-controlled chamber (35% RH, 25 °C) for over 7 days. Once dried, the films were easily delaminated from the Petri dish.

Torque Viscometry of CNF/CMC, CNF/XG, and CNF/aPAM Pastes. A Brabender torque rheometer (Plasti-Corder PL 2100 Electronic Torque Rheometer, C. W. Brabender, South Hackensack, NJ), equipped with roller head blades, was used to measure the viscosity−shear rate dependence of the CNF/CMC, CNF/XG, and CNF/aPAM pastes. Examples from the literature[33,35−40] have shown that small-chambered torque rheometers are a practical means to obtain the viscosity−shear rate behavior of polymer-based systems. Recently, Santi et al.[40] proposed that the torque−temperature dependence must be characterized to correct the final viscosity data for viscous dissipation effects. The analysis used in this study was slightly modified from the process described by Costakis et al.,[41] and the details are explained below.

For the analysis, the sample chamber was loaded to 70% of the total volume (60 cm^3) with the CNF/processing aid paste and mixed at an initial temperature of 21 °C with a roller speed of 10 rpm for 7 min. Once the torque and temperature were stable, the torque data were collected at 21, 28, and 32 °C for 3 min to characterize the torque−temperature dependence. The viscosity temperature sensitivity constant (b) was obtained from the exponential fit of the torque versus temperature graph. This constant was used in eq 1 to correct the measured viscosity data for temperature increases because of viscous dissipation

$$\Gamma(T) = \Gamma(T_o)\exp[-b(T - T_o)] \tag{1}$$

where $\Gamma(T)$ is torque as a function of temperature, T is the set temperature, and T_o is the measured temperature of the blend.[40,41] After the torque−temperature analysis, the sample was removed and replaced with another sample from the same batch to reduce the drying effects. Then, the temperature was set to 28 °C, and the roller speed was set to 10 rpm. The torque data were collected at 10, 20, 30, 50, 70, and 90 rpm in 3 min intervals to obtain the torque−rpm dependence of each paste. The calibration and analysis suggested by Bousmina et al.[37] were applied to obtain the shear rate and viscosity data. The details for the calibration process and calculation of the effective equivalent internal radius (R_i) are explained in detail by Costakis et al.[41] Once R_i was obtained, it was used in the following equations to calculate the shear rate from eq 2 and viscosity from eq 3 for each paste.

$$\dot{\gamma} \approx \frac{2\pi N}{\ln\left(\frac{R_c}{R_i}\right)} \tag{2}$$

$$\eta = \frac{\Gamma}{N}\frac{\left(\frac{R_c}{R_i}\right)^2 - 1}{8\pi^2 L R_c^2 \cdot (1 + g^2)} \tag{3}$$

The log(viscosity) dependence on log(shear rate) was linearly fit to obtain the power law index (n) and melt consistency index (m) for each paste.

In addition to this analysis, a controlled shear stress response rheometry was performed using a Malvern Bohlin Gemini HR Nano Rheometer with a cup and bob fixture (C25 DIN 53019). Aliquots of the highly loaded extrusion pastes (CNF/CMC, CNF/XG, and CNF/aPAM) were diluted with DI water to 1 wt %. The diluted suspensions were loaded using a syringe; roughly, 12 mL was added. A gap of 150 μm was set for all experiments. A pre-shear of 1 s^{-1} for 60 s was applied to erase the loading history. A shear range of 0.1−

https://dx.doi.org/10.1021/acsapm.0c00477
ACS Appl. Polym. Mater. 2020, 2, 3365−3377

100 s^{-1} was probed with an integration time of 10 s, a delay time of 10 s, and 30 sample points. The temperature of the fixture was controlled at 25 °C.

Zeta Potential. Suspensions for zeta potential analysis were prepared identically to the suspensions intended for centrifugation with a processing aid-to-CNF ratio of 0.05:1 (except for aPAM with a ratio of 0.025:1 because of the high viscosity). These suspensions were then diluted with deionized water to a concentration of 0.024% (w/v) and shear-mixed at 4500 rpm for 3 min. A transfer pipette was used to transfer the dilute suspensions into disposable capillary cells. The CNF content in the dilute suspension allowed for a good number of particles for scattering (>100,000 counts/s), and a lower processing aid content did not significantly increase the viscosity of the suspensions. The viscosity of each different suspension was not measured but assumed to be that of water. The pH of each suspension was measured with a pH meter (HANNA Instruments). Unless stated otherwise, the pH of the suspensions prepared was 6.4. A total of six zeta potential measurements were collected using a Zetasizer Nano ZS (Malvern Panalytical) analyzer and disposable folded capillary cells (DTS1070). The average value of all six measurements was taken to be the final zeta potential, and the standard deviation (STD) was calculated for the measurements. Quality criteria were met for all tests, yet the count rate varied when testing the pure CNF suspension.

Extruder Configuration and Extrusion Parameters. The pastes were extruded using the Brabender torque rheometer (ATR) unit with an attached single-screw extruder unit (L/D = 25, barrel diameter of 1.9 cm, and four independent heating zones) (Figures S6 and S7). A conventional 3:1 compression screw was used to extrude all pastes. An adjustable 5.08 cm wide slot die/sheet die was attached to the end of the extruder to form the extrudates into rectangular sheets. The initial width of the slot die (i.e., wet sheet thickness) was adjusted to be 1.131 mm by using feeler gauges. For all extrusions performed, ∼75 g of the paste was loaded into the feeder section with the use of an in-house-made plunger, as they were too viscous to be gravity-fed (Figure S6). Roughly ∼61 cm long sheets were produced for each experiment performed. Unless stated differently, all the extrusions were performed at a screw speed of 7 rpm and a temperature of 25 °C in all heating zones (low temperature setting in Figure S7). The friction generated at these low rpm values was not enough to significantly raise the temperature during extrusion. The pressure before the die, screw torque, and barrel temperature were recorded during extrusion.

Sample Preparation for Mechanical Testing. The ∼61 cm long wet extrudates were cut into smaller ∼116 mm long segments. Subsequently, two smaller segments were sandwiched between two stainless steel meshes and two silicone sheets (Figure S8) and pressed at a temperature of 126 °C for 30 min using a hydraulic-heated laboratory press model no. 3690 (Carver). After drying, the tensile test dogbones were cut from the sheets in the machine direction, following ASTM D638. The total dogbone length was 92 mm, with a neck width of 4.80 mm and a gauge length of 26.40 mm. The thickness varied between 0.211 mm and 0.298 mm based on the solid concentration. The dogbones were cut using a laser cutter (Muse Desktop Laser, Full Spectrum LASER, Las Vegas, NV) equipped with a 10.6 μm CO_2 40 W laser. One to three passes (varied based on the solid content of the paste) at 35% power and 100% speed were used to cut the samples and reduce damage. For sample conditioning, the cut samples were placed in a desiccator at ∼25% RH for at least 2 days before mechanical testing. The dogbones were tested in tension using an electromechanical testing machine (MTS Insight) equipped with a 2000N load cell and serrated film clamps. To avoid sample slippage during testing, sandpaper was added at the grips. For all samples tested, a preload force of 1 N was applied. The cross-head speed was set to 1 mm/min. The ambient humidity could not be controlled and varied between 30 and 50% RH, yet large batches of samples (6−24 samples) were tensile-tested on the same day to reduce variation among the data sets. Once tested, the ultimate stress or strength (MPa) and strain to failure (%) were taken from the last data point collected. Young's modulus was determined through the steepest slope method. Strain was measured based on cross-head displacement without the use of an extensometer. The obtained mechanical testing data were collected by the built-in software (TestWorks4). Grip compliance was measured using a thick 1020 steel specimen, and the sample data were adjusted accordingly. For density measurement, smaller specimens of 8 mm by 8 mm were cut from the same sheet as that of the dogbones. A caliper and a micrometer were used to measure the width and thickness of the squares, whereas the mass was measured using an analytical balance (VWR).

Lastly, the cast CNF films were cut with the same laser cutter but with a reduced 25% power and a single pass. The dogbone specimens were smaller (37 mm long, a neck width of 1 mm, and a gauge length of 6.50 mm) yet still followed ASTM D638 (type IV) with a thickness of 80 ± 4 μm. The specimens were tested using a dynamic mechanical analyzer model Q800 from TA Instruments (TA Instruments Inc., Wood Dale, IL). A strain-controlled mode was used with a preload force of 0.010 N and a strain rate of 0.5 mm/min until failure.

Thermogravimetric Analysis. Thermogravimetric analysis (TGA) was performed using a thermogravimetric analyzer model Q50 from TA Instruments (TA Instruments Inc., Wood Dale, IL). Roughly, 40−50 mg of the cast CNF or warm-pressed extrudates were loaded into a platinum pan. Prior to testing, all the samples were preconditioned for over a week at 25% RH. The samples were tested in the temperature range of 25−300 °C at a heating rate of 10 °C/min in an oxygen atmosphere.

Scanning Electron Microscopy. The fractured surfaces of the tensile-tested specimens were imaged using a Quanta 650 FEG field emission electron microscope. The fractured surfaces were positioned normal to the aluminum stub and secured using a carbon tape. The samples were sputter-coated (SPI sputter coater) with a platinum−gold target for 60 s. No polishing or sanding was used. The samples were imaged at 4 keV and a spot size of 4. The working distance varied between 9 and 10 mm for the highest resolution.

Statistical Analysis for Mechanical Testing. Unless otherwise stated, six sample units were tested for each CNF/processing aid paste sample shown in the bar graphs. The laser-cut specimens were visually inspected for any excessive burn marks or surface defects before performing mechanical testing. Only those with excessive defects or any edge burn marks were removed from the sample set. Additional samples were processed to account for any removed sample unit in a sample set. Statistical analysis was performed using OriginPro. The error bars shown represent 1 STD away from the mean value for the data set. A normality test was performed on the data sets to verify a normal distribution followed by Student's t test (95% confidence interval) to determine the statistical similarity/difference among data sets or an analysis of variance (ANOVA) with the same confidence level.

RESULTS AND DISCUSSION

Extrusion of Pure CNF and Processing Aid Selection. With the primary goal of processing 100% pure CNF sheets, initial attempts to extrude the CNF were performed without the use of any processing aid. The extrusion of pure CNF was assessed at six different solids concentrations: 3.1, 10, 17, 20, 24, and 30 wt % and at two different extrusion temperatures of 25 and 90 °C (see Figure S7). Results show that all pure CNF pastes with a solid concentration of 3.1, 10, 17, 20, and 24 wt % experienced significant amounts of dewatering. The dewatering raised the total solid concentration of the pastes to roughly ∼85 wt %, which clogged the slot die and stopped the process (Figure S9a). The increased solid loading easily raised the die pressures to the extruder's maximum limitation of ∼69 MPa. Furthermore, because of the lack of drainage/solvent ports in the barrel, the extracted water traveled opposite to the extrusion direction and pooled in the hopper region (Figure S9b). The pooling of water caused rehydration of the newly fed material which was unable to push the dewatered material

https://dx.doi.org/10.1021/acsapm.0c00477
ACS Appl. Polym. Mater. 2020, 2, 3365−3377

at the slot die. Lastly, CNF at ∼30 wt % experienced dewatering but to a much lower extent and was capable of being extruded into short sheet segments with an average length of ∼90 mm. The longest produced sheet with a length of ∼330 mm is shown in Figure 1. That said, clogging still occurred during the extrusion operations at this solid concentration.

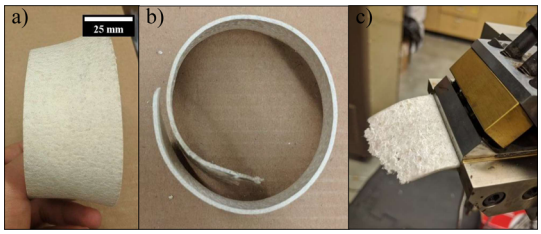

Figure 1. Extrudate of pure CNF originally at 30 wt % solid concentration: (a) front view (width of ∼5 cm), (b) side view (thickness of ∼1.1 mm), and (c) coming out of the slot die. The extrudate had a solid concentration of ∼85 wt % coming out of the die. The total length of the sheet was ∼330 mm. The sheet was very fragile and easily broken into pieces.

The reduced dewatering observed for pure CNF at 30 wt % facilitated its processability. On the other hand, hornification could have also restricted the ability of the CNF to re-form hydrogen bonds and homogenize (i.e., retake shape) once the conveyed material reached the slot die for forming.[42] The inability to retake shape after exiting the die caused an excessive amount of agglomeration/inhomogeneity in the sheet, which made the structure very fragile. For pure CNF, a lower solid concentration could possibly be needed for forming and homogenization (i.e., fiber swelling) to occur during extrusion. Additionally, for all CNF loadings assessed, using higher processing temperatures of 90 °C seemed to exacerbate all the problems observed for lower processing temperatures of 25 °C. Hence, all subsequent extrusions were performed at a temperature of 25 °C.

Because of the prevailing dewatering problems, a processing aid was desired. Thickeners, viscosifiers, and gelling agents have been used to viscosify suspensions and could serve to aid water retention.[43] Table 1 shows the selected candidates as well as the surface charges and acronyms which will be used throughout the report.

As a first approach, the water-retention ability or water-holding capacity of the suspensions containing viscosifiers was assessed through centrifugation. This approach is essentially an accelerated separation column test which bypasses particle diffusion and hence the long wait times associated with standard gravity separation. Additionally, if separation occurs at the pressures associated with the centrifugal forces, as they are not as high as in an extruder, then the processing aid will not be suitable. Centrifugation showed that suspensions containing CMC, XG, or aPAM at a dry weight ratio of aid to CNF of 0.1:1 did not experience any perceivable water separation or solid−liquid separation (Figure S10). All the other suspensions (not marked with an asterisk, Table 1) experienced a slight level of dewatering (∼2 to 3 mL of water extracted; MC, HEMC, HEC, GG, CG-λ, CP940, and TG) or had a water separation behavior similar to that of pure CNF (∼20 mL of water separated; KM, AS, CS, PEI, and PAA). Similar results are produced for suspensions with a reduced ratio of processing aid to CNF of 0.05:1, where CMC-, XG-, and aPAM-containing suspensions did not dewater, yet all other suspensions experienced dewatering at an even greater extent. Processing aids like KM formed irreversible gels when mixed with water, which could not be fully incorporated into CNF; hence, KM was not further studied.[44] The water retention provided by CMC, XG, and aPAM could not necessarily be linked to the surface charge, as other negatively charged surface polymers did not suppress dewatering to the same extent (e.g., TG, CP940, CG-λ, and PAA). Similarly, although higher molecular weight (M_w) polymers often lead to higher viscosities, making it hard to separate species, the water retention of CNF/aid suspensions could not be directly linked to the M_w of the aid. For example, CMC-containing suspensions did not dewater and had a much lower M_w (∼150,000 to 180,000) when compared to XG (M_w ∼ 300,000 to 7.5 × 10^6),[30] aPAM (in the millions),[29] or even CP940 (M_w ∼7 × 10^5 to 4 × 10^9)[45] which did dewater.

Table 1. Thickeners, Viscosifiers, and Gelling Agents Assessed Based on Their Water-Retention Ability When Incorporated into a CNF Slurry (∼3 wt % Solids)[a]

processing aid	charge at pH 6−7	acronym
methyl cellulose	nonionic	MC
hydroxyethyl methyl cellulose	nonionic	HEMC
hydroxyethyl cellulose	nonionic	HEC
guar gum	nonionic	GG
konjac glucomannan	nonionic	KM
amphoteric starch	+ & −	AS
cationic starch	+	CS
poly(ethyleneimine)	+	PEI
polyacrylic acid sodium salt	−	PAA
carrageenan-lambda	−	CG-λ
Carbopol 940	−	CP940
tragacanth gum	−	TG
Carboxymethyl cellulose sodium salt*	−	CMC
Xanthan gum*	−	XG
Anionic polyacrylamide*	−	aPAM

[a]All the selected processing aids are soluble in water at room-temperature conditions. *Processing aids which fully suppressed water separation.

In order to further gauge the stability of the centrifuged suspensions and possibly explain the observed water-retention behavior, zeta potential was measured on dilute (0.024% w/v) suspensions of CNF and processing aid. The results showed that CMC-, XG-, aPAM-, CP940-, CG-λ-, and PAA- containing suspensions experienced the largest magnitude of charge. CMC, XG, aPAM, and CG-λ all lowered the zeta potential below −50 mV, with the largest increase in charge being caused by the addition of CMC (ξ = −58 ± 5.63 mV). This represents a relatively large increase in stability when compared to pure CNF with ξ = −29.8 ± 4.35 mV, which tends to phase-separate at room-temperature conditions and without any centrifugation. Aids like TG, CS, and AS did not have any effect on the surface charge when compared to pure CNF, whereas HEC, MC, and HEMC all decreased it, hence theoretically reducing stability (Figure 2).

Zeta potential results matched with the centrifugation behavior observed for CMC, XG, and aPAM, indicating that colloidal stability is the origin of the water-retention results. However, this supposition did not match for other processing aids. For example, MC-, HEMC-, HEC-, and GG-containing suspensions experienced the same low level of dewatering as

https://dx.doi.org/10.1021/acsapm.0c00477
ACS Appl. Polym. Mater. 2020, 2, 3365−3377

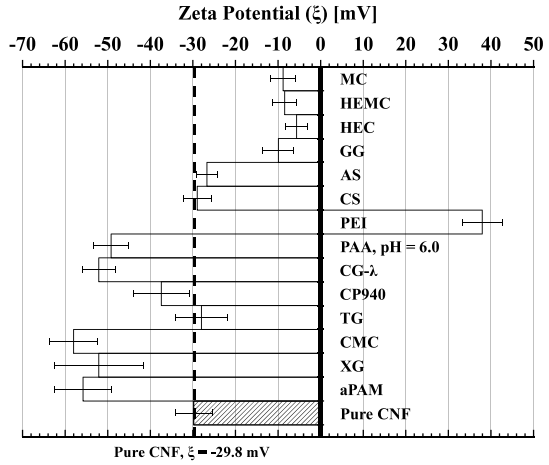

Figure 2. Zeta potential of pure CNF and CNF/aid suspensions which were diluted with DI water to a concentration of 0.024% (w/v). The dashed line shown is referenced to the mean of the pure CNF zeta potential (ξ = −29.8 mV). Six measurements were performed for each case and the average was calculated. The error bars represent 1 STD away from the mean. The pH of all the samples was measured to be 6.4, except for PAA that had a pH of 6.0.

those containing CG-λ (ξ = −52.1 ± 3.83 mV) and CP940 (ξ = −37.4 ± 6.59 mV) when compared against pure CNF. Furthermore, the PAA-containing suspension (ξ = −49.2 ± 4.09 mV) experienced the same dewatering behavior as pure CNF. Strongly positively charged polymers like PEI flipped the sign of the surface charge yet did not provide water retention during centrifugation trials. Thus, although improved suspension stability can make it more difficult to separate species, it alone cannot directly explain the dewatering behavior of CNF/aid suspensions. Lastly, it is important to point out that although it is indeed possible to achieve no water separation during centrifugation for the slightly dewatering suspensions (i.e., those that contain MC, HEMC, HEC, GG, CG-λ, CP940, or TG) by increasing the amount of polymer (e.g., aid/CNF ratio of 0.15:1 or 0.2:1), the intent of this work is to produce extruded sheets with the highest CNF purity. Hence, only CMC, XG, and aPAM were selected for further studies.

Extrusion of CNF/CMC, CNF/XG, and CNF/aPAM Pastes. Based on an initial extrusion trial of three different solid loadings (∼3, ∼7.6, and ∼15 wt %) of a CNF/CMC paste (0.1:1 of aid to CNF), it was determined that a total solid concentration of ∼15 wt % is needed to form cohesive sheets. Lower solid concentrations would extrude, yet the extrudate was too watery and not cohesive enough to be transported or handled (Video S2). Based on the results, a ∼15 wt % total solid concentration was selected for all extrusion pastes unless otherwise stated.

To achieve a ∼15 wt % concentration, the watery CNF/processing aid suspensions (∼3 wt %) could be air-dried for roughly 40 days (see Figure S11). However, to circumvent the long drying times, concentrated pastes containing CMC, XG, and aPAM were prepared by using a standard polymer Banbury-style high shear mixer, the procedure for which is explained in detail in the Experimental Section. The high shear mixing process utilized a bottom-up approach to achieve higher solid loadings by using vendor pre-dewatered pure CNF (∼23 wt % solids instead of a ∼3 wt % slurry). The needed processing aid and water were then added to tune the final solid concentration. In the literature, a similar approach was used to produce ultrahigh consistency pulp/biomass pastes (20 to 40 wt %) with the addition of processing aids or water-soluble polymers like CMC, HPMC, XG, agar, and HPC.[46] A validation analysis of the mixing process used is presented in the Supporting Information.

The extrusion of CNF/CMC (0.05:1 of aid to CNF), CNF/XG (0.05:1), or CNF/aPAM (0.013:1) pastes failed because of dewatering at the slot die and did not form homogeneous sheets (Figure S12). This shows that although centrifugation is a good initial screening test for processing aids (e.g., a list of 15 candidates was reduced to 3, Table 1), it clearly does not replicate the complex pressure profiles and shear forces in an extruder or the behavior of highly loaded pastes. On the other hand, CNF/CMC and CNF/XG pastes at 0.1:1 and CNF/aPAM pastes at 0.026:1 of aid to CNF did not dewater and were capable of being formed into wet sheets. Extrudates/sheets with an average width of ∼5.1 cm and a wet thickness of 1.46 ± 0.05 mm were processed for each paste type, CNF/CMC, CNF/XG, and CNF/aPAM (Figure 3 and Video S3). It is important to note that the length of the extrudate was only limited by the amount of material at hand and by the lack of collection rolls.

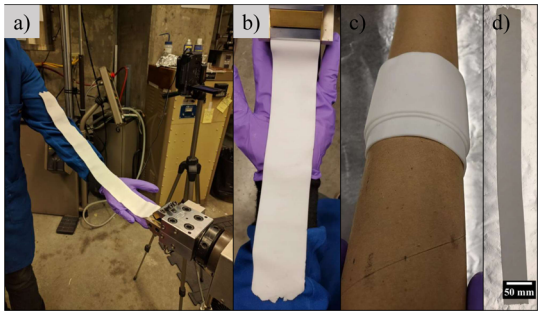

Figure 3. Wet CNF/CMC sheet single-screw extrusion (a), wet CNF/CMC extrudate (∼15 wt % total solids) exiting the rectangular sheet die (b), extrudate collected on a cardboard roll (c), and derolled extrudate laid flat on top of an aluminum foil (d).

Wet sheet production rates at a screw speed of 7 rpm were in the range of 0.45 ± 0.02 kg/h (or 0.07 ± 0.002 kg/h dry), whereas the maximum possible production rate was found to be 7.45 ± 0.47 kg/h (or 1.14 ± 0.072 dry) at a screw speed of 110 rpm for CNF/CMC pastes (15.32 wt % solids). Figure S13 shows a plot of the production rate (kg/h) versus screw speed (rpm) for a CNF/CMC (0.1:1) paste at ∼15 wt %. There was a strong (R^2 = 0.997) linear relationship between the extrusion/delivery rate and the screw speed until the maximum screw speed (120 rpm) was reached, which experienced a decrease in the rate to 6.24 ± 0.12 kg/h (0.96 ± 0.02 kg/h dry). The reduction of the delivery rate could possibly be caused by the shear thinning response of the paste. If the shear is high enough to cause shear thinning of the material pressed against the barrel walls, the screw's ability to transport a material will be hindered.[47] It is expected that the maximum possible production rates will depend on both the processing aid type and the total solid concentration as the rheological response will change (as seen in the next section). The obtained processing rates are much lower than typical industrial single-screw extrusion lines with a throughput of approximately 40 kg/h at 122 rpm (approximation by Fang et al.[48] for processing LDPE), yet current efforts only employ a laboratory-scale extruder with a relatively small barrel diameter

https://dx.doi.org/10.1021/acsapm.0c00477
ACS Appl. Polym. Mater. 2020, 2, 3365−3377

(1.9 cm) and small width (5.08 cm) sheet die. It is also important to point out that at all the screw speeds, there was neither a "shark skin" nor a ridged pattern observed at the extrudate's surface. It is possible that the lubricating water layer or the depletion layer that forms between two phase materials and solid surfaces suppressed the stick-slip behavior common in capillary dies.[49,50] On the other hand, a small amount of die swell was observed as the extrudates were on average slightly thicker (1.46 ± 0.05 mm) than the set die gap width (1.13 mm).

When compared against laboratory processing techniques (e.g., solution casting), the major benefit that comes from using the proposed methodology (a shear mixer to produce pastes and an extruder to continuously process sheets) is the significant reduction in processing time. Additionally, when compared to the previously reported extruded cellulose nanocomposites, the proposed methodology allows for the processing of sheets with very high solids and CNF loading (up to ∼91 wt % CNF and ∼9 wt % processing aid) compared to nanocomposites (a maximum of 20 wt % CNF content).[22−25,51] Processing nearly pure CNF parts conserves 100% of the inherent mechanical properties of CNF. Lastly, problems dealing with matrix incompatibility and matrix selection are essentially eliminated.

When comparing wet extrudates, it was found that CNF/CMC extrudates were the most homogeneous and contained no perceivable surface or bulk defects such as pinholes, aggregation, inhomogeneity, and so forth (Figure 4a). CNF/XG extrudates contained some pinholes and agglomerated structures, whereas CNF/aPAM extrudates contained numerous defects (Figure 4b,c). Collectively, for all wet extrudates, larger defects were partly transferred to the fully dry state after pressing and heating (Figure 4d−i), which ultimately lead to lower mechanical performance, as shown in the Statistical Analysis for Mechanical Testing section. Additionally, similar defect patterns were observed inside of the sheet die after extrusion and during cleaning (Figure S14).

Rheological Analysis of Pure CNF, CNF/CMC, CNF/XG, and CNF/PAM Pastes. Rheological analysis of highly concentrated pastes was carried out on a Brabender torque rheometer. The viscosity−temperature sensitivity constants (b, used to correct the measured torque data) were measured for each paste and are shown in Table 2. From here, the torque and roller speed were converted to viscosity and shear rate through eqs 1−3 and plotted in Figure 5.

Figure 5 shows the log(viscosity) dependence on log(shear rate) at 28 °C for 15.32 wt % pastes containing CMC, XG, aPAM, and pure CNF. The solid lines correspond to linear curve fits, with all $R^2 > 0.98$. The power law index (or shear thinning exponent, n) and melt consistency index (m) were calculated from the power law fits and are shown in Table 2. Figure 5 and the values in Table 2 show that the addition of CMC suppressed the shear thinning behavior when compared to that of pure CNF. The power law index increased from n = 0.13 for pure CNF to n = 0.42 for CNF/CMC at 15.32 wt %. For the CNF/XG paste, issues because of slippage at the mixing blades started to occur at ∼50 to 70 rpm (data points are not filled in to signify unreliable data, Figure 5), and hence the power law index and consistency index could not be reliably calculated or compared (note n is negative, Table 2, Figure 5, and Video S4). Slippage was most likely caused by the highly shear thinning rheological behavior of XG when compared to other thickeners. This behavior is possibly caused

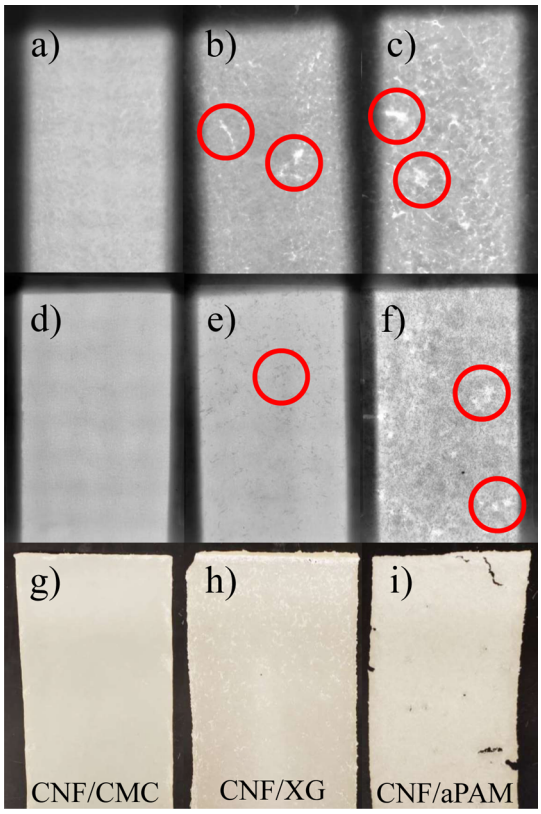

Figure 4. Wet extrudates of CNF/CMC (a), CNF/XG (b), and CNF/aPAM (c) pastes at ∼15 wt %, pressed and heated to fully dry sheets of CNF/CMC (d,g), CNF/XG (e,h), and CNF/aPAM (f,i). A strong backlight was used to illuminate samples and highlight the defects like aggregation/aggregates or pinholes. A few of the observed defects are circled in red. Panels (a) through (f) were set to a gray scale to better appreciate the defects, whereas panels (g−i) were not color modified. The width of the sheets was ∼51 mm. The faint square pattern observed in some of the sheets originates from the LED light arrangement on the back of the sheets.

by the weak association between XG molecules and their relatively stiff conformation.[52] XG molecules take on a stiff right-hand fivefold helical conformation with a large hydrodynamic size and with a persistence length, q > 100 nm.[52−54] This is in contrast to more flexible linear molecules like CMC (q ∼ 10−30 nm) that take on a ribbon-like conformation and are also characterized by a pseudoplastic behavior.[52] The conformation of XG allows for higher viscosities at lower shear rates. Slippage also occurred for CNF/aPAM yet in a more significant manner at lower rpm values (≤5 rpm). Hence, CNF/aPAM could not be characterized using the Brabender rheometer. One rheological study showed that adding trace amounts (10 g/m^3) of aPAM to paper pulp highly increased the elongational viscosity and drainage time while keeping the shear viscosity the same.[55] Perhaps, for the CNF/aPAM pastes prepared (15.32 wt % total solids with the aid-to-CNF ratio of 0.026:1), the high aPAM concentration (∼4500 g/m^3) could have influenced the shear viscosity as it does the elongational viscosity for trace amounts in dilute suspensions, thus exacerbating slippage.

When compared to the extrudates (Figure 4), it appears that pastes with a reduced shear thinning behavior or stronger Newtonian behavior present less defects and hence have a greater sheet homogeneity. A plausible reason for the fact that

https://dx.doi.org/10.1021/acsapm.0c00477
ACS Appl. Polym. Mater. 2020, 2, 3365−3377

Table 2. Paste Concentrations and Rheological Constants Obtained from Torque Rheometry Analysis[a]

paste type	total solids [wt %]	aids [wt %]	CNF [wt %]	H_2O [wt %]	b [°C^{-1}]	R^2	n	log(m)	R^2
pure CNF	15.32	0	15.32	84.68	0.0085	0.944	0.13	3.533	1.000
	30	0	30	70	0.0145	0.982	0.06	4.470	1.000
CNF/CMC	15.32	1.39	13.93	84.68	0.0119	0.941	0.42	2.991	0.995
	19	1.73	17.27	81	0.0107	0.963	0.30	3.359	0.998
	25	2.27	22.72	75	0.0040	0.729	0.26	3.494	0.999
CNF/XG	15.32	1.39	13.93	84.68	0.0049	0.722	−0.31	3.666	0.982

[a]A dry weight ratio of 0.1:1 (aid/CNF) was used for all pastes.

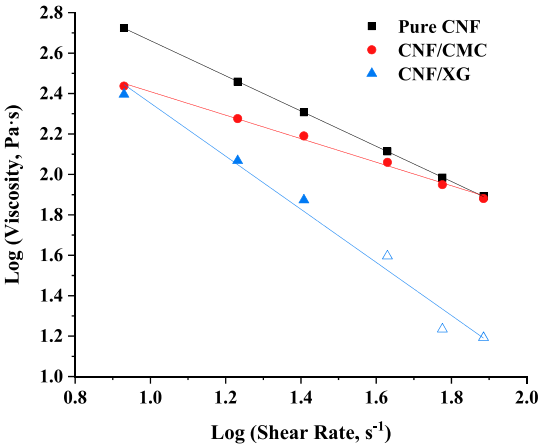

Figure 5. log(viscosity)−log(shear rate) dependence of pure CNF, CNF/CMC, and CNF/XG pastes with an aid-to-CNF ratio of 0.1:1 measured on the torque rheometer at 28 °C. The power law index is calculated by n = (slope + 1), whereas the consistency index is the intercept point. All the analyzed pastes and pure CNF had a solid concentration of 15.32 wt %. Unfilled points represent unreliable data because of slipping or sticking to the mixing blades.

having a stronger Newtonian behavior reduces sheet defects is that during forming, the complex shear profiles inside the die will have a weaker effect on the final part shape (i.e., reduced shear sensitivity of the paste). In fact, this is why in conventional commodity polymer extrusion lines there is a unique die for each polymer being processed. Individual die designs account for the vastly different flow characteristics (e.g., shear thinning exponent (n), melt flow index (MI), and die swell) of the polymers and ensure high-quality parts.[56] That said for the prepared pastes, CMC appears to impart both good rheological properties and strong dispersion to CNF pastes and allows for successful extrusion without defects.

For all shear rates studied and for both processing aids added (CMC and XG), there was a marked decrease of the apparent viscosity of the pastes when compared to pure CNF (Figure 5). Classically, in synthetic polymer extrusion, the same effect is caused by the processing aids that act as internal lubricants. For example, polyglycerol ester (C_{16} to C_{22}) fatty acids are added to reduce the characteristic high melt viscosity of poly(vinyl chloride), poly(propylene), or acrylonitrile−butadiene−styrene.[57] For CNF/aid pastes, the decrease in viscosity is possibly caused by the reduction of fibril−fibril contacts and fibril−fibril friction as part of the dispersed/dissolved polymer molecules adsorb to fibrils and improve dispersion.[58] More specifically, for CMC, the frictional reduction and dispersion effects have been studied extensively for more dilute papermaking suspensions (∼1 to ∼3 wt % total solids) that contain CMC as a wet-end additive in the dispersed phase or adsorbed CMC onto the pulp fibers.[59−62] Because CNFs have the same surface chemistry as bleached kraft pulp often used in papermaking suspensions, it is believed that the reported effects were carried over to the extrusion pastes. Contrary to CMC, XG has not been studied as an additive in papermaking suspensions, yet similar effects could be occurring in terms of fibril−fibril friction and contact reduction as well as adsorption.

Typical rotational shear rate-controlled rheometry with a cup and bob fixture served as a secondary analysis/comparison and was performed on dilute suspensions (1 wt %) of CNF/CMC, CNF/XG, CNF/aPAM, and pure CNF because of the high viscosity of highly loaded pastes making them unmeasurable in our system (Figure S15). The obtained trends for the suspensions matched those obtained for the highly loaded pastes (Figure 5). For example, adding CMC reduced the shear thinning behavior (n = 0.11 for pure CNF and n = 0.30 for CNF/CMC, Figure S15). In contrast to the torque rheometry analysis, CNF/XG and CNF/aPAM watery suspensions could be analyzed without slippage. The behavior of CNF/XG and CNF/aPAM was similar in that both suppressed the shear thinning behavior (n = 0.26 for CNF/XG and n = 0.24 for CNF/aPAM) when compared to pure CNF. The apparent viscosity of CNF/XG and CNF/aPAM was also lower than that of CNF/CMC at all shear rates studied. Interestingly, a power law transition in pure CNF at ∼5 s^{-1} disappeared with the addition of processing aids. Although the reason is not clear, it was deemed beyond the scope of this paper. Nonetheless, these results only serve as indirect comparisons to the torque rheometer results, and greater importance is given to highly loaded pastes which achieve the concentrations desired for extrusion.

Additional analysis, using the torque rheometer, of the two higher concentration (∼19 and ∼25 wt %) CNF/CMC pastes (at 0.1:1) showed that a higher total solid concentration reduced the power law index and hence increased the shear thinning response (n = 0.42 for ∼15 wt %, n = 0.3 for ∼19 wt %, and n = 0.26 for ∼25 wt %, Figure 6 and Table 2). As expected, there is also a general trend that a higher solid concentration leads to higher apparent viscosities for all shear rates probed because of the higher density of particle interactions. It is important to note that the only "successful" extrudate of pure CNF at ∼30 wt % showed an order of magnitude higher viscosities when compared to ∼25 wt % CNF/CMC and a stronger shear thinning behavior (n = 0.06) when compared to the ∼15 wt % pure CNF paste (n = 0.13). It is also important to point out that while testing pure CNF samples (∼15 and ∼30 wt %) slight dewatering occurred, which might have affected the rheological response; this was not quantified as the amount of water lost only coated the surfaces of the mixer.

Because of the lack of literature on steady-state rheometry of highly loaded CNF pastes, the results were indirectly

https://dx.doi.org/10.1021/acsapm.0c00477
ACS Appl. Polym. Mater. 2020, 2, 3365−3377

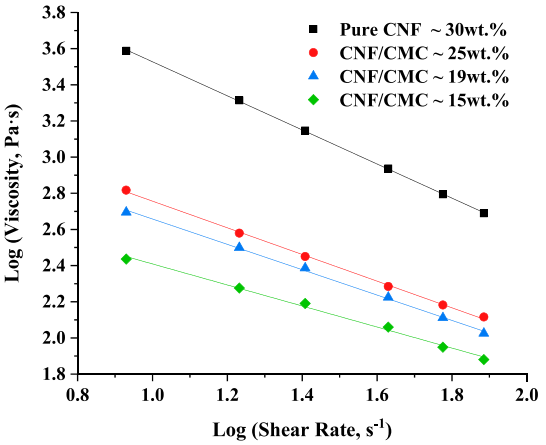

Figure 6. log(viscosity)−log(shear rate) dependence of CNF/CMC pastes with solid loadings of ~15, ~19, and ~25 wt % and pure CNF at ~30 wt % measured on a torque rheometer at 28 °C. The processing aid-to-CNF ratio for the evaluated pastes was 0.1:1 (dry weight).

compared with that of corn stover biomass pastes tested under dynamic conditions. Highly loaded corn stover pastes (20 wt % solids) tested using a vane rheometer showed a shear thinning behavior similar to that of CNF pastes, with a linearly decreasing complex viscosity (η^*) ranging from 10,000 Pa·s (0.3 Hz) to 50 Pa·s (100 Hz).[63,64] The measured elastic (G') modulus was on average an order of magnitude higher than the storage (G'') modulus, and both were found to be relatively insensitive to frequency. The reported solid-like behavior ($G' \gg G''$) of corn stover can be explained in terms of the increased particle interactions (i.e., higher solids). This solid-like behavior is expected to be intensified for highly loaded pure CNF pastes as the particle sizes are much smaller than corn stover biomass (i.e., more interactions). On the other hand, Samaniuk et al. showed that CMC was an excellent corn stover processing aid when compared to other aids like poly(ethylene)oxide, nonionic polyacrylamide (PAM), and XG.[34,65] Adding 2 wt % CMC achieved a reduction of yield stress (τ_y) of ~67% (~55 to ~18 kPa) for 25 wt % corn stover pastes.[34] The obtained results are consistent with previously stated theories regarding the reduction of fibril−fibril contacts and friction through the processing aid adsorption to the surfaces of the insoluble particles in the paste.[66] The reduction in friction reduces fiber entanglements or fiber flocs and explains the stronger Newtonian behavior seen for CNF/CMC pastes (Figures 5 and 6). The fibril−fibril friction theory could also explain why as the solid loading increases for the CNF/CMC pastes the shear thinning exponent (n) decreases from n = 0.42 for ~15 wt % to n = 0.26 for ~25 wt % solids (Table 2).

Mechanical Analysis of CNF/CMC, CNF/XG, and CNF/aPAM Sheets. Mechanical testing of the pressed and dried extrudates with an aid-to-CNF dry weight ratio of 0.1:1 showed that CNF/CMC sheets outperformed CNF/XG sheets in terms of ultimate strength (110.6 ± 7.30 and 60.1 ± 19.5 MPa, respectively) and strain to failure (1.80 ± 0.08 and 0.75 ± 0.26%, respectively), as shown in Figure 7a,c. These results were not surprising as CNF/XG sheets contained more defects than CNF/CMC sheets (Figure 4). Because of the significantly higher level of defects, CNF/aPAM sheets were not tested mechanically as the properties are expected to be much lower when compared to any of the other extruded sheets (Figure 4). Additionally, there seems to be no significant difference between the mean densities for the cast CNF films and the extrudates of CNF/CMC and CNF/XG (one-way ANOVA: $F_{2,16}$ = 3.47, P = 0.056, R^2 = 0.302, Figure 7d). The density of the sample groups is better appreciated in the boxplots shown in Figure S16. In the literature, CNF films have been reported to form extensive nanoporous networks,[67] which explains the lower densities observed for both cast CNF films and CNF/aid extrudates when compared to crystalline cellulose (1.5 to ~1.6 g/cm^3).[4]

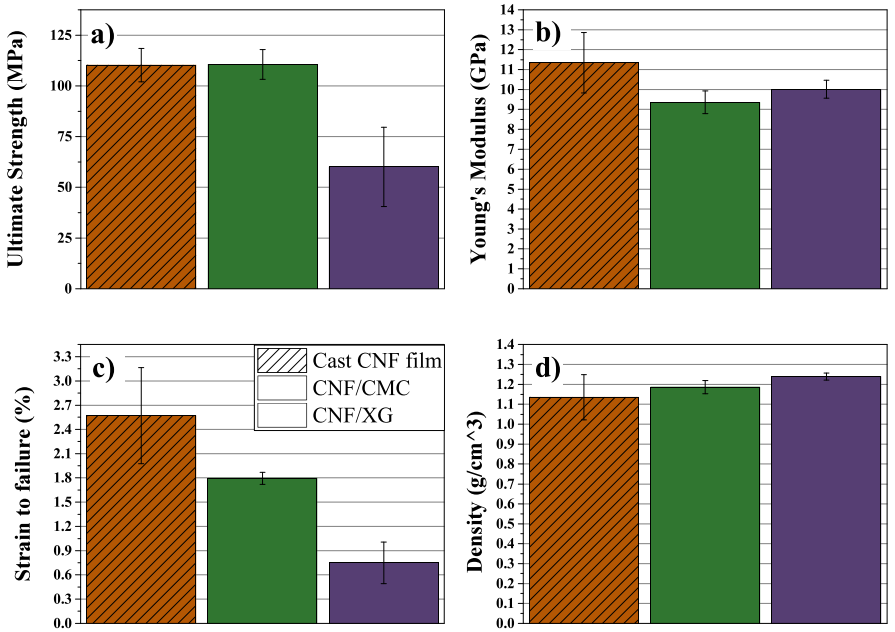

Figure 7. Tensile testing response; ultimate strength (a), Young's modulus (b), strain to failure (c), and density (d) for cast CNF films, and extruded CNF/CMC and CNF/XG sheets with a processing aid-to-CNF ratio of 0.1:1. The error bars represent 1 STD away from the mean for all graphs. The sample size for the cast CNF films was 7, whereas the sample size for CNF/CMC and CNF/XG sheets was 6.

https://dx.doi.org/10.1021/acsapm.0c00477
ACS Appl. Polym. Mater. 2020, 2, 3365−3377

When compared against cast CNF films prepared through typical solution casting, the extruded CNF/CMC sheets were statistically the same in terms of ultimate strength (110 ± 8.2 MPa for cast CNF films versus 110.6 ± 7.30 MPa for extruded CNF/CMC sheets) and density (1.13 ± 0.11 g/cm^3 for cast CNF films versus 1.19 ± 0.03 g/cm^3 for CNF/CMC). Collectively, for both CNF/CMC and CNF/XG, the extruded sheet's strain to failure was lower than that of cast CNF films (2.57 ± 0.6%), yet this is probably an artifact of the constrained drying applied to the extruded sheets versus the room-temperature unconstrained/free drying used for cast CNF films. In terms of Young's modulus, all the extruded sheets were statistically similar to cast CNF films (Figure 7b).

The observed mechanical performance of CNF/CMC extrudates is lower than those typically reported for cast TEMPO-oxidized CNF films, with the ultimate strength values reaching ∼300 MPa.[68] Yet, unoxidized CNF is generally cheaper (e.g., ∼11 vs ∼328 cents/g, varies per supplier).[31] Previous works have also demonstrated that ultimate strength values of up to ∼207 MPa can be achieved via wet-stacking and heated pressing of CNF sheets.[20] That said, CNF/CMC extrudates were stronger and stiffer than typical polystyrene and nylon 6,6, which achieve ultimate strength values of ∼11 and ∼45 MPa and modulus of ∼1.8 and ∼1.4 GPa, respectively.[20]

TGA of the pressed and heated extrudates revealed a similar degradation behavior between CNF/aPAM and the ∼30 wt % pure CNF extrudate with a pronounced weight loss, reaching over 2% at 100 °C (Figure S17). On the other hand, CNF/CMC and CNF/XG sheets behaved more like cast CNF films with a less pronounced weight loss, reaching 1% at 100 °C. Further details are presented in the Supporting Information. Scanning electron microscopy (SEM) analysis of the extruded sheets and cast CNF films did not reveal any additional information (Figure S18). All the tested sheets and films presented a paper-like layered structure, with the fibrils pointing toward the tensile direction. The fractured surfaces looked similar to a previous work on thicker multilayered neat CNF sheets.[20] Table S2 summarizes the mechanical response, including the specific strength and specific modulus of all the extruded and pressed sheets as well as cast CNF films. Furthermore, preliminary attempts at calendering the wet extrudates of CNF/CMC showed that full extrudate consolidation can be achieved, and a more translucent sheet is developed (Figure S19). The mechanical properties of the calendered sheets were not evaluated, but a higher density and ultimate strength is expected.

Higher processing aid concentrations were also probed in order to better gauge the effect of the processing aid on the mechanical properties. The results showed that adding CMC at a ratio of 0.15:1 (aid-to-CNF) lowered all the mechanical properties (Figure S20), possibly because of the excess CMC surrounding the CNF fibrils. Surprisingly, the addition of XG at a ratio of 0.15:1 (aid to CNF) improved all the mechanical properties when compared to the pressed sheets with a XG-to-CNF ratio of 0.1:1 (Figure S21). The addition of more XG appeared to reduce macroscopic defects like pinholes and aggregates, possibly because of the improved CNF dispersion. A comparison between CNF/CMC at 0.1:1 and CNF/XG at 0.15:1 is shown in Figure S22.

CONCLUSIONS

In this work, the processing of CNF sheets through conventional single-screw extrusion was presented and assessed. The results show that common problems associated with conventional single-screw extrusion of pure CNF such as dewatering, clogging, and aggregation were completely suppressed with the addition of low concentrations of processing aids like CMC, XG, and aPAM. It was found that the processing aids could be successfully incorporated into vendor pre-dewatered pure CNF using standard polymer high shear mixing in a much faster and more controlled process than air drying to produce highly loaded (∼25 wt % solids) extrudable CNF/aid pastes. The processed CNF/aid pastes could be extruded at rates of up to 7.45 ± 0.47 kg/h (or 1.14 ± 0.072 dry) without any significant introduction of surface defects (e.g., shark skin) and without limitations on the final length. Out of the assessed processing aids, CMC significantly reduced the shear thinning response and appears to impart a strong dispersion to CNF pastes, which allows for a successful extrusion without defects like aggregates and pinholes. The stronger Newtonian response brought by the addition of CMC could have been possibly caused by a reduction of fibril−fibril friction, which is believed to reduce fibril entanglements or fiber flocs and agglomeration. Additionally, press drying and tensile testing of the processed CNF/CMC extrudates revealed equivalent mechanical properties in terms of ultimate strength, density, and modulus when compared to cast CNF films prepared by typical solution casting, proving that the mechanical properties were conserved through extrusion. Lastly, calendering of the wet extrudates showed that full consolation can be achieved, which eliminates the need to use discrete pressing steps.

More broadly, the results obtained show that it is possible to utilize common polymer processing methods for CNF from the beginning to end of the processing chain, allowing the potential to significantly increase the production rate and lower the cost. Banbury high-shear mixing, extrusion, and calendering provide an elegant way to both continuously process CNF and take advantage of the already developed polymer melt-processing industry, while, at the same time, taking advantage of their relatively lower cost as compared to typical papermaking production methods. Though the work performed employed the use of a single-screw extruder, it is envisioned that the use of other more advanced extruder configurations, such as twin-screw extruders that can handle more viscous polymer melts allowing more concentrated CNF/aid pastes (above 25 wt % total solids) or single-screw extruders with mixing stages or twin-screw mixing extruders allowing continuous mixing of the processing aid in line with extrusion in a single step, would add utility, as is performed commercially with polymer melts, currently.

ASSOCIATED CONTENT

Supporting Information

The Supporting Information is available free of charge at https://pubs.acs.org/doi/10.1021/acsapm.0c00477.

Recorded Brabender mixing response for processing of highly loaded CNF pastes for extrusion, validation analysis of the shear mixing process, photographs of processed pastes, composition summary for prepared pastes, extruder configuration and processing parameters, pressing configuration for extrudate consolidation,

https://dx.doi.org/10.1021/acsapm.0c00477
ACS Appl. Polym. Mater. 2020, 2, 3365−3377

drying behavior for air-dried pastes, correlation between the extrusion output rate and screw speed, rotational viscometry analysis of CNF suspensions, SEM of the fractured surfaces of tensile-tested specimens, complete mechanical response summary of all tested samples, preliminary CNF sheet calendering result photographs, TGA of the pressed extrudates, and mechanical response of pastes prepared with a higher processing aid content (PDF)
(AVI)
(AVI)
(AVI)
(AVI)

AUTHOR INFORMATION

Corresponding Author

Jeffrey P. Youngblood − *School of Materials Engineering, Purdue University, West Lafayette, Indiana 47907, United States;* orcid.org/0000-0002-8720-8642; Phone: +1 765-496-2294; Email: jpyoungb@purdue.edu; Fax: +1 765 494-1204

Authors

Sami M. El Awad Azrak − *School of Materials Engineering, Purdue University, West Lafayette, Indiana 47907, United States;* orcid.org/0000-0002-6384-7212

William J. Costakis − *School of Materials Engineering, Purdue University, West Lafayette, Indiana 47907, United States*

Robert J. Moon − *Forest Products Laboratory, United States Forest Service, Madison, Wisconsin 53726, United States;* orcid.org/0000-0001-9526-0953

Gregory T. Schueneman − *Forest Products Laboratory, United States Forest Service, Madison, Wisconsin 53726, United States;* orcid.org/0000-0002-6390-5240

Complete contact information is available at: https://pubs.acs.org/10.1021/acsapm.0c00477

Funding

The authors thank the US Endowment and the Public-Private Partnership for Nanotechnology (grant number: 109217) and Army Research Office for funding this research (grant number: W911NF-17-0203).

Notes

The authors declare no competing financial interest.

ACKNOWLEDGMENTS

The authors would like to thank Dr. Carlos Martinez for the advice given with regard to the zeta potential measurements.

REFERENCES

(1) Lieder, M.; Rashid, A. Towards Circular Economy Implementation: A Comprehensive Review in Context of Manufacturing Industry. *J. Cleaner Prod.* **2016**, *115*, 36−51.
(2) Kaur, G.; Uisan, K.; Ong, K. L.; Ki Lin, C. S. Recent Trends in Green and Sustainable Chemistry & Waste Valorisation: Rethinking Plastics in a Circular Economy. *Curr. Opin. Green Sustain. Chem.* **2018**, *9*, 30−39.
(3) Shogren, R.; Wood, D.; Orts, W.; Glenn, G. Plant-Based Materials and Transitioning to a Circular Economy. *Sustain. Prod. Consum.* **2019**, *19*, 194−215.
(4) Moon, R. J.; Martini, A.; Nairn, J.; Simonsen, J.; Youngblood, J. Cellulose Nanomaterials Review: Structure, Properties and Nanocomposites. *Chem. Soc. Rev.* **2011**, *40*, 3941−3994.
(5) Turbak, A. F.; Snyder, F. W.; Sandberg, K. R. Microfibrillated Cellulose, a New Cellulose Product: Properties, Uses, and Commercial Potential. *J. Appl. Polym. Sci.* **1983**, *37*, 815.
(6) Herrik, F. W. Process For Preparing Microfibrillated Cellulose. U.S. Patent 4,481,077 A, 1984.
(7) Moon, R. J.; Schueneman, G. T.; Simonsen, J. Overview of Cellulose Nanomaterials, Their Capabilities and Applications. *JOM* **2016**, *68*, 2383−2394.
(8) Mondal, S. Review on Nanocellulose Polymer Nanocomposites. *Polym.-Plast. Technol. Eng.* **2018**, *57*, 1377−1391.
(9) Foster, E. J.; Moon, R. J.; Agarwal, U. P.; Bortner, M. J.; Bras, J.; Camarero-Espinosa, S.; Chan, K. J.; Clift, M. J. D.; Cranston, E. D.; Eichhorn, S. J.; Fox, D. M.; Hamad, W. Y.; Heux, L.; Jean, B.; Korey, M.; Nieh, W.; Ong, K. J.; Reid, M. S.; Renneckar, S.; Roberts, R.; Shatkin, J. A.; Simonsen, J.; Stinson-Bagby, K.; Wanasekara, N.; Youngblood, J. Current Characterization Methods for Cellulose Nanomaterials. *Chem. Soc. Rev.* **2018**, *47*, 2609−2679.
(10) Lin, N.; Dufresne, A. Nanocellulose in Biomedicine: Current Status and Future Prospect. *Eur. Polym. J.* **2014**, *59*, 302−325.
(11) Roman, M. Toxicity of Cellulose Nanocrystals: A Review. *Ind. Biotechnol.* **2015**, *11*, 25−33.
(12) Axelsson, L.; Franzen, M.; Ostwald, M.; Berndes, G.; Lakshmi, G.; Ravindranath, N. H. Perspective: Jatropha Cultivation in Southern India: Assessing Farmers' Experiences. *Biofuels, Bioprod. Biorefin.* **2012**, *6*, 246−256.
(13) de Assis, C. A.; Iglesias, M. C.; Bilodeau, M.; Johnson, D.; Phillips, R.; Peresin, M. S.; Bilek, E. M.; Rojas, O. J.; Venditti, R.; Gonzalez, R. Cellulose Micro- and Nanofibrils (CMNF) Manufacturing - Financial and Risk Assessment. Biofuels, Bioprod. *Biorefining* **2018**, *12*, 251−264.
(14) Rol, F.; Vergnes, B.; El Kissi, N.; Bras, J. Nanocellulose Production by Twin-Screw Extrusion: Simulation of the Screw Profile to Increase the Productivity. *ACS Sustainable Chem. Eng.* **2020**, *8*, 50−59.
(15) Clarkson, C. M.; El Awad Azrak, S. M.; Chowdhury, R.; Shuvo, S. N.; Snyder, J.; Schueneman, G.; Ortalan, V.; Youngblood, J. P. Melt Spinning of Cellulose Nanofibril/Polylactic Acid (CNF/PLA) Composite Fibers For High Stiffness. *ACS Appl. Polym. Mater.* **2019**, *1*, 160−168.
(16) Chowdhury, R. A.; Clarkson, C.; Youngblood, J. Continuous Roll-to-Roll Fabrication of Transparent Cellulose Nanocrystal (CNC) Coatings with Controlled Anisotropy. *Cellulose* **2018**, *25*, 1769−1781.
(17) Sehaqui, H.; Liu, A.; Zhou, Q.; Berglund, L. A. Fast Preparation Procedure for Large, Flat Cellulose and Cellulose/Inorganic Nanopaper Structures. *Biomacromolecules* **2010**, *11*, 2195−2198.
(18) Chowdhury, R. A.; Clarkson, C. M.; Shrestha, S.; El Awad Azrak, S. M.; Mavlan, M.; Youngblood, J. P. High-Performance Waterborne Polyurethane Coating Based on a Blocked Isocyanate with Cellulose Nanocrystals (CNC) as the Polyol. *ACS Appl. Polym. Mater.* **2020**, *2*, 385−393.
(19) Clarkson, C. M.; El Awad Azrak, S. M.; Schueneman, G. T.; Snyder, J. F.; Youngblood, J. P. Crystallization Kinetics and Morphology of Small Concentrations of Cellulose Nanofibrils (CNFs) and Cellulose Nanocrystals (CNCs) Melt-Compounded into Poly(Lactic Acid) (PLA) with Plasticizer. *Polymer* **2020**, *187*, 122101.
(20) El Awad Azrak, S. M.; Clarkson, C. M.; Moon, R. J.; Schueneman, G. T.; Youngblood, J. P. Wet-Stacking Lamination of Multilayer Mechanically Fibrillated Cellulose Nanofibril (CNF) Sheets with Increased Mechanical Performance for Use in High-Strength and Lightweight Structural and Packaging Applications. *ACS Appl. Polym. Mater.* **2019**, *1*, 2525−2534.
(21) Wang, Q.; Yao, Q.; Liu, J.; Sun, J.; Zhu, Q.; Chen, H. Processing Nanocellulose to Bulk Materials: A Review. *Cellulose* **2019**, *26*, 7585−7617.
(22) Hietala, M.; Mathew, A. P.; Oksman, K. Bionanocomposites of Thermoplastic Starch and Cellulose Nanofibers Manufactured Using Twin-Screw Extrusion. *Eur. Polym. J.* **2013**, *49*, 950−956.

(23) Gong, G.; Pyo, J.; Mathew, A. P.; Oksman, K. Tensile Behavior, Morphology and Viscoelastic Analysis of Cellulose Nanofiber-Reinforced (CNF) Polyvinyl Acetate (PVAc). *Composites, Part A* **2011**, *42*, 1275−1282.
(24) Jonoobi, M.; Harun, J.; Mathew, A. P.; Oksman, K. Mechanical Properties of Cellulose Nanofiber (CNF) Reinforced Polylactic Acid (PLA) Prepared by Twin Screw Extrusion. *Compos. Sci. Technol.* **2010**, *70*, 1742−1747.
(25) Oksman, K.; Aitomaki, Y.; Mathew, A. P.; Siqueira, G.; Zhou, Q.; Butylina, S.; Tanpichai, S.; Zhou, X.; Hooshmand, S. Review of the Recent Developments in Cellulose Nanocomposite Processing. *Composites, Part A* **2016**, *83*, 2−18.
(26) Picker, K. M.; Hoag, S. W. Characterization of the Thermal Properties of Microcrystalline Cellulose by Modulated Temperature Differential Scanning Calorimetry. *J. Pharm. Sci.* **2002**, *91*, 342−349.
(27) Borsoi, C.; Zimmernnam, M. V. G.; Zattera, A. J.; Santana, R. M. C.; Ferreira, C. A. Thermal Degradation Behavior of Cellulose Nanofibers and Nanowhiskers. *J. Therm. Anal. Calorim.* **2016**, *126*, 1867−1878.
(28) Nechyporchuk, O.; Belgacem, M. N.; Pignon, F. Current Progress in Rheology of Cellulose Nanofibril Suspensions. *Biomacromolecules* **2016**, *17*, 2311−2320.
(29) Hubbe, M. A.; Nanko, H.; McNeal, M. R. Retention Aid Polymer Interactions with Cellulosic Surfaces and Suspensions: A Review. *BioResources* **2009**, *4*, 850−906.
(30) Kang, K. S.; Pettitt, D. J.; Xanthan; Gellan; Welan; Rhamsan, A. N. In *Industrial Gums: Polysaccharides and Their Derivatives*, 3rd ed.; Whistler, R. L., Bemiller, J. N., Eds.; Academic Press, Inc., 2012; pp 341−397.
(31) University of Maine. Order Nanocellulose. https://umaine.edu/pdc/nanocellulose/order-nanocellulose/ (accessed 2020-03-15).
(32) Desmaisons, J.; Boutonnet, E.; Rueff, M.; Dufresne, A.; Bras, J. A New Quality Index for Benchmarking of Different Cellulose Nanofibrils. *Carbohydr. Polym.* **2017**, *174*, 318−329.
(33) Xu, X.; Hilmas, G. E. The Rheological Behavior of Ceramic/Polymer Mixtures for Coextrusion Processing. *J. Mater. Sci.* **2007**, *42*, 1381−1387.
(34) Samaniuk, J. R.; Scott, C. T.; Root, T. W.; Klingenberg, D. J. Rheological Modification of Corn Stover Biomass at High Solids Concentrations. *J. Rheol.* **2012**, *56*, 649−665.
(35) Goodrich, J. E.; Porter, R. S. A Rheological Interpretation of Torque-rheometer Data. *Polym. Eng. Sci.* **1967**, *7*, 45−51.
(36) Beeaff, D. R.; Hilmas, G. E. Rheological Behavior of Coextruded Multilayer Architectures. *J. Mater. Sci.* **2002**, *37*, 1259−1264.
(37) Bousmina, M.; Ait-Kadi, A.; Faisant, J. B. Determination of Shear Rate and Viscosity from Batch Mixer Data. *J. Rheol.* **1999**, *43*, 415−433.
(38) Blyler, L. L.; Daane, J. H. An Analysis of Brabender Torque Rheometer Data. *Polym. Eng. Sci.* **1967**, *7*, 178−181.
(39) Marquez, A.; Quijano, J.; Gaulin, M. A Calibration Technique to Evaluate the Power-Law Parameters of Polymer Melts Using a Torque-Rheometer. *Polym. Eng. Sci.* **1996**, *36*, 2556−2563.
(40) Santi, C. R.; Hage, E. H., Jr.; Correa, C. A.; Vlachopoulos, J. Torque Viscometry of Molten Polymers and Composites. *Appl. Rheol.* **2009**, *19*, 13148.
(41) Costakis, W. J.; Schlup, A. P.; Youngblood, J. P.; Trice, R. W. Aligning α-Alumina Platelets via Uniaxial Pressing of Ceramic-Filled Polymer Blends for Improved Sintered Transparency. **2019**, *103*, 3500. DOI: 10.1111/jace.17044, Accepted.
(42) Fernandes Diniz, J. M. B.; Gil, M. H.; Castro, J. A. A. M. Hornification—Its Origin and Interpretation in Wood Pulps. *Wood Sci. Technol.* **2004**, *37*, 489−494.
(43) Kulkarni, V. S.; Shaw, C.; Kulkarni, V. S.; Shaw, C. Use of Polymers and Thickeners in Semisolid and Liquid Formulations. In *Essential Chemistry for Formulators of Semisolid and Liquid Dosages*; Academic Press, 2016; pp 43−69.
(44) Saha, D.; Bhattacharya, S. Hydrocolloids as Thickening and Gelling Agents in Food: A Critical Review. *J. Food Sci. Technol.* **2010**, *47*, 587−597.
(45) Brady, J.; Drig, T.; Lee, P. I.; Li, J. X. Polymer Properties and Characterization. In *Developing Solid Oral Dosage Forms: Pharmaceutical Theory and Practice*, 2nd ed.; Qiu, Y., Zhang, G. G. Z., Mantri, R. V., Chen, Y., Yu, L., Eds.; Elsevier Inc., 2017; pp 181−223.
(46) Scott, C. T. Pulp Extrusion at Ultra-High Consistencies: Selection of Water-Soluble Polymers for Process Optimization. *TAPPI Fall Technical Conference and Trade Fair*, 2002; pp 1621−1629.
(47) Lafleur, P. G.; Vergnes, B. Single-Screw Extrusion. *Polymer Extrusion*; ISTE Ltd. and John Wiley & Sons, Inc., 2014; pp 37−108.
(48) Fang, S.; Chen, L.; Zhu, F. Studies on the Theory of Single Screw Plasticating Extrusion. Part II: Non-plug Flow Solid Conveying. *Polym. Eng. Sci.* **1991**, *31*, 1117−1122.
(49) Derakhshandeh, B.; Kerekes, R. J.; Hatzikiriakos, S. G.; Bennington, C. P. J. Rheology of Pulp Fibre Suspensions: A Critical Review. *Chem. Eng. Sci.* **2011**, *66*, 3460−3470.
(50) Dealy, J. M.; Wang, J. Role of Rheology in Melt Processing. *Melt Rheology and its Applications in the Plastics Industry*; Springer, 2013; pp 205−260.
(51) Herrera, N.; Mathew, A. P.; Oksman, K. Plasticized Polylactic Acid/Cellulose Nanocomposites Prepared Using Melt-Extrusion and Liquid Feeding: Mechanical, Thermal and Optical Properties. *Compos. Sci. Technol.* **2015**, *106*, 149−155.
(52) Williams, P. A.; Phillips, G. O. Introduction to Food Hydrocolloids. *Handbook of Hydrocolloids*, 2nd ed.; Woodhead Publishing Limited, 2009; pp 1−22.
(53) Sworn, G. Xanthan Gum. *Handbook of Hydrocolloids*; Woodhead Publishing, 2009; pp 186−203.
(54) Imeson, A. In *Food Stabilisers, Thickeners and Gelling Agents*; Imeson, A., Ed.; John Wiley & Sons, Ltd, 2009.
(55) Lee, P. F. W.; Lindstrom, T. Effect of High Molecular Mass Anionic Polymers on Paper Sheet Formation. *Nord. Pulp Pap Res. J.* **1989**, *4*, 61−70.
(56) Ellwood, K. R. J.; Papanastasiou, T. C.; Wilkes, J. O. Three-dimensional Streamlined Finite Elements: Design of Extrusion Dies. *Int. J. Numer. Methods Fluid.* **1992**, *14*, 13−24.
(57) Hall, L. K.; Rosen, M. Polyglycerol Plastic Lubricants. U.S. Patent 4,481,324 A, 1984.
(58) Butchosa, N.; Zhou, Q. Water Redispersible Cellulose Nanofibrils Adsorbed with Carboxymethyl Cellulose. *Cellulose* **2014**, *21*, 4349−4358.
(59) Liimatainen, H.; Haavisto, S.; Haapala, A.; Niinimaki, J. Influence of Adsorbed and Dissolved Carboxymethyl Cellulose on Fibre Suspension Dispersing, Dewaterability, and Fines Retention. *BioResources* **2009**, *4*, 321−340.
(60) Yan, H.; Lindstrom, T.; Christiernin, M. Some Ways to Decrease Fibre Suspension Flocculation and Improve Sheet Formation. *Nord. Pulp Pap. Res. J.* **2006**, *21*, 36−43.
(61) Beghello, L.; Lindstrom, T. The Influence of Carboxymethylation on the Fiber Flocculation Process. *Nord. Pulp Pap. Res. J.* **1998**, *13* (). DOI: DOI: 10.3183/npprj-1998-13-04-p269-273.
(62) Watanabe, M.; Gondo, T.; Kitao, O. Advanced Wet-End System with Carboxymethyl-Cellulose. *Tappi* **2004**, *3*, 35−45.
(63) Stickel, J. J.; Knutsen, J. S.; Liberatore, M. W.; Luu, W.; Bousfield, D. W.; Klingenberg, D. J.; Scott, C. T.; Root, T. W.; Ehrhardt, M. R.; Monz, T. O. Rheology Measurements of a Biomass Slurry: An Inter-Laboratory Study. *Rheol. Acta* **2009**, *48*, 1005−1015.
(64) Samaniuk, J. R.; Wang, J.; Root, T. W.; Scott, C. T.; Klingenberg, D. J. Rheology of Concentrated Biomass. *Korea Aust. Rheol. J.* **2011**, *23*, 237−245.
(65) Samaniuk, J. R.; Scott, C. T.; Root, T. W.; Klingenberg, D. J. Effects of Process Variables on the Yield Stress of Rheologically Modified Biomass. *Rheol. Acta* **2015**, *54*, 941−949.
(66) Schmid, C. F.; Klingenberg, D. J. Properties of Fiber Flocs with Frictional and Attractive Interfiber Forces. *J. Colloid Interface Sci.* **2000**, *226*, 136−144.

https://dx.doi.org/10.1021/acsapm.0c00477
ACS Appl. Polym. Mater. 2020, 2, 3365−3377

(67) Bardet, R.; Reverdy, C.; Belgacem, N.; Leirset, I.; Syverud, K.; Bardet, M.; Bras, J. Substitution of Nanoclay in High Gas Barrier Films of Cellulose Nanofibrils with Cellulose Nanocrystals and Thermal Treatment. *Cellulose* **2015**, *22*, 1227−1241.
(68) Saito, T.; Hirota, M.; Tamura, N.; Kimura, S.; Fukuzumi, H.; Heux, L.; Isogai, A. Individualization of Nano-Sized Plant Cellulose Fibrils by Direct Surface Carboxylation Using TEMPO Catalyst under Neutral Conditions. *Biomacromolecules* **2009**, *10*, 1992−1996.

https://dx.doi.org/10.1021/acsapm.0c00477
ACS Appl. Polym. Mater. 2020, 2, 3365−3377